

Quantitative Reaction Cascades of Ninhydrin in the Solid State

Gerd Kaupp,* M. Reza Naimi-Jamal, and Jens Schmeyers^[a]

Abstract: Crystalline ninhydrin (**1**) undergoes waste-free solid-state cascade reactions with dimedone, L-proline, three *o*-phenylenediamines, *o*-mercaptoaniline, two ureas, three thioureas, and methyl 3-aminocrotonate. The yields are quantitative and give pure crystalline products without workup just by milling stoichiometric mixtures of the crystalline reagents. The structures of the new and the previously obtained products with lower yields from solutions are established or confirmed by spectroscopic data and density functional cal-

culations at the B3LYP/6-31G* level. The success of 3- and 4-cascade reactions in the crystal without melting is unusual and of unmatched atom economy. They are mechanistically investigated with atomic force microscopy techniques (AFM) on six different faces of **1** when *o*-phenylenediamine was the re-

agent (substitution, elimination, cyclization, elimination) and interpreted on the basis of known crystal structure data. Strict correlations to the crystal packings are observed. The characteristic surface features grow to μm heights in some cases at distances of 0.5 mm from the contact edge of the reacting crystals. The waste-free and easy syntheses of highly functionalized (C=O; O-H; C=N) heterocycles or of a tetraketone are also of interest for synthetic use.

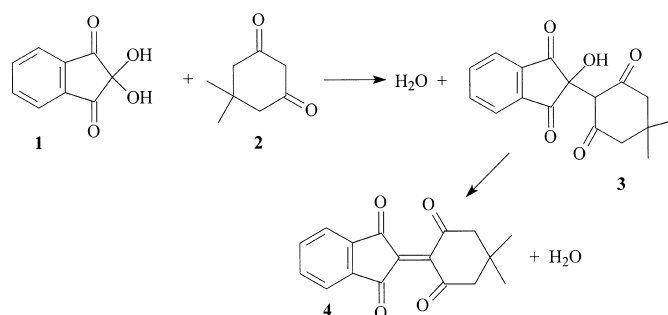
Keywords: environmentally benign • heterocycles • ninhydrin • scanning probe microscopy • solid-state reactions

Introduction

Gas-solid and solid-solid reactions profit from the crystal packing and have been mechanistically investigated.^[1] They require long-range molecular movements (phase rebuilding), phase transformation into the product lattice and creation of fresh surface by crystal disintegration. Frequently they run to completion with highest selectivity and give 100 % yield under moderate reaction conditions without any necessity for work-up. Even multistage cascade reactions were quantitative in the solid state, a fact that provides unsurpassed efficiency in terms of environmental protection and savings of both labor and resources. We now extended those principles to versatile reactions of ninhydrin **1** in 2-, 3- and 4-cascades of various reaction types.

Results

Quantitative one-step condensation: The solid state reaction of ninhydrin **1** with dimedone **2** in a ball-mill proceeds only as a one-step condensation to give **3** with 100 % yield (Scheme 1). Compound **3** has previously been synthesized in



Scheme 1. Quantitative condensation of ninhydrin with dimedone.

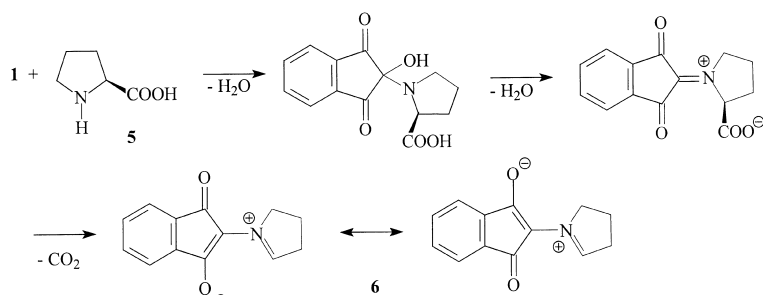
solution with 82 % yield.^[2] No dehydration was observed in the solid state to yield **4** even with gaseous trimethylamine or hydrogen chloride or *p*-toluenesulfonic acid. Anyhow, the liquid-state synthesis of **4** in anhydrous dioxane with trifluoroacetic anhydride and pyridine^[3] gains importance, as **3** is now more easily accessible without producing any waste. Such reluctance for solid-state elimination of water was not typical for all condensation reactions of ninhydrin in the solid state.

Quantitative 3-cascade with proline: The presumed wealth of amino acids in solid-state reactions has not yet been exploited so far. It is thus of high interest that L-proline **5** reacts quantitatively in a 3-cascade (substitution, elimination, decarboxylation) with **1** to give the versatile azomethine ylide **6** (Scheme 2) waste-free and in quantitative yield. Again, **6** can

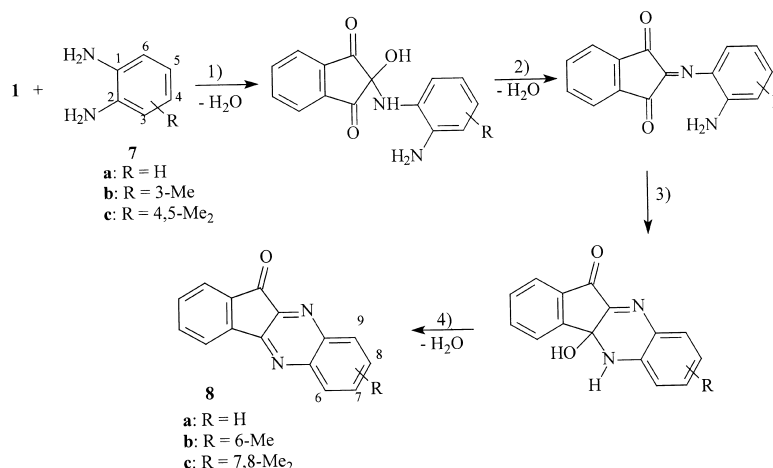
[a] Prof. Dr. G. Kaupp, Dr. M. R. Naimi-Jamal, Dr. J. Schmeyers
University of Oldenburg, FB Chemie, Organische Chemie I
Postfach 2503, 26111 Oldenburg (Germany)
Fax: (+49) 441-7983-409
E-mail: kaupp@kaupp.chemie.uni-oldenburg.de

be synthesized in solution but only with 82 % yield.^[4] It has been used for 1,3-dipolar cyclo-additions.^[5] The zwitterionic structure of **6** is secured by the symmetry of the aromatic proton resonances, the presence of an iminium H ($\delta = 9.24$) and of an iminium C ($\delta = 213.78$) in the NMR spectra. In support of this structure, density functional theory (DFT) calculations at the B3LYP/6-31G* level find the cyclized valence tautomers by 15.25 (spiroaziridine) or 17.49 kcal mol⁻¹ (oxazoline) higher in energy content.

Quantitative 4-cascades with *o*-phenylenediamines: Various solid *o*-phenylenediamines **7** react quantitatively with solid ninhydrin **1** in 4-cascades (substitution, elimination, cyclization, elimination) to give the indenoquinoxaline ketones **8** (Scheme 3). Similar reactions proceed in solution with yields of 61 % to almost quantitative.^[6] The presumed sequence



Scheme 2. Quantitative 3-cascade in the solid-state reaction of ninhydrin with L-proline.



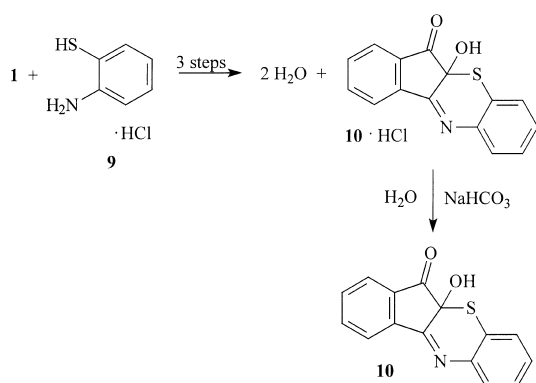
Scheme 3. Quantitative solid-state 4-cascades of ninhydrin with *o*-phenylenediamines.

Abstract in German: Kristallines Ninhydrin (**1**) geht mit Dimedon, L-Prolin, drei *o*-Phenylendiaminen, *o*-Mercaptoanilin, zwei Harnstoffen, drei Thioharnstoffen und 3-Aminocrotonsäuremethylester abfallfreie Kaskadenreaktionen im festen Zustand ein. Die Ausbeuten sind quantitativ und geben reine kristalline Produkte beim Vermahlen stöchiometrischer Mischungen der kristallinen Reaktanden, ohne dass reinigende Aufarbeitung erforderlich wäre. Die Konstitution der neuen und früher aus Lösungen mit schlechterer Ausbeute erhaltenen Produkte werden mittels spektroskopischer Daten und Dichtefunktional Theorie Rechnungen auf dem B3LYP/6-31G* Niveau begründet und bestätigt. Der gute Erfolg der 3- und 4-Kaskaden-Reaktionen im Kristall ohne flüssige Phase ist ungewöhnlich und von überragender Atom-Ökonomie. Sie werden daher mittels Kraftmikroskopie (AFM) auch mechanistisch untersucht. Dies gelingt mit *o*-Phenylendiamin auf sechs verschiedenen kristallographischen Flächen von **1** (Substitution, Eliminierung, Cyclisierung, Eliminierung). Die Interpretation gelingt auf Grundlage der bekannten Röntgenstrukturanalyse: Es wird die strikte Korrelation zur Kristallpackung bestätigt. Die charakteristischen Oberflächenstrukturen wachsen auf **1** in einigen Fällen bis zur Mikrometer-Höhe obwohl der Reagenzkristall 0.5 mm entfernt aufliegt. Die abfallfreien und besonders einfachen Synthesen hochfunktionalisierter (C=O; O-H; C=N) Heterocyclen oder eines Tetraketons sind auch von synthetischem Interesse.

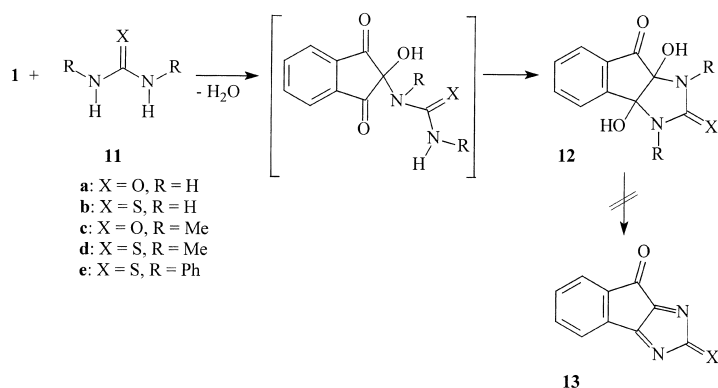
of events (substitution, elimination, addition, and elimination) allows for a rationalization of the orientation selectivity found. While **7a** and **7c** have no orientational choice (see products **8a** and **8c**), **7b** yields the 6-Me isomer **8b** exclusively (75 % in solution^[6a]) obviously for steric reasons in the primary substitution step. The structures of the compounds **8** have been derived from the NMR data and by comparison with the known isomers from the solution reactions. The possibility of a symmetric diketo spiro-aminal structure is excluded by the asymmetry in the NMR spectra and the lack of N–H vibrations in the IR spectrum.

Quantitative 3-cascade with *o*-mercaptoaniline hydrochloride: Stoichiometric reactions of solid **1** with solid *o*-mercaptoaniline hydrochloride (**9**) gives the salt **10**·HCl (Scheme 4) in quantitative yield by substitution, cyclization, and elimination. The free base **10** has a very low solubility in water and can thus be obtained in quantitative yield by a NaHCO₃ treatment. Similar reactions in solution were reported to provide only 60 % yield.^[7] Compound **10** is remarkably stable: It does not form a spiro-N/S-acetal upon heating up to its melting point at 227 °C.

Quantitative 2-cascades with ureas: Ureas (**11**) and more easily thioureas (**11**) are well suited for substitution and addition to **1** (Scheme 5). The interesting heterocyclic bis-



Scheme 4. Quantitative solid-state 3-cascade of ninhydrin and *o*-mercaptoaniline.

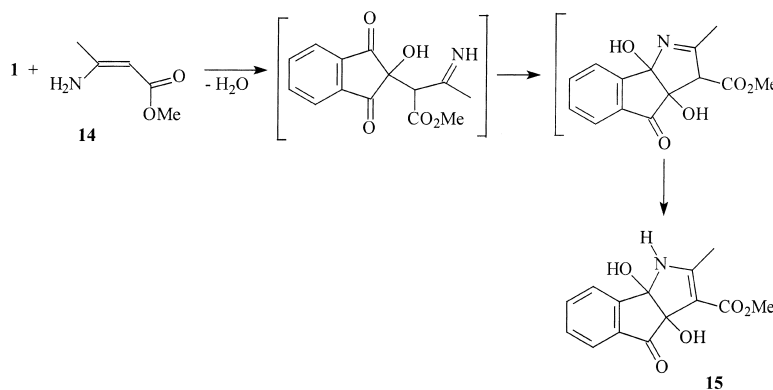


Scheme 5. Quantitative 2-cascades of ninhydrin and (thio)ureas in the solid state.

N/O-semiacetals **12** are stable compounds that form with 100% yield in all cases studied (**a–e**). Some of these have been previously prepared in solution with inferior yields (Table 1). It is remarkable that neither **12a** nor **12b** eliminate water during heating in the DSC/TGA experiments up to the melting points. Even HCl (gas) or *p*-toluenesulfonic acid (solid) do not produce the anticipated elimination products **13** in the solid state. However, the now waste-free access to the compounds **12** opens certainly numerous versatile possibilities for further syntheses using their α -hydroxyketone, α -amino-ketone and *N/O*-semiacetal functionalities. The structures **12** are secured by the NMR spectra which exclude symmetrical diketo spiro[5,4]aminal structures.

Quantitative 3-cascade with methyl 3-aminocrotonate:

The solid enaminoester **14** reacts quantitatively with **1** in stoichiometric ball-mill runs without intermediate liquid phase to give the heterocyclic building block **15** with α -hydroxyketone and *N/O*-semiaminal functionality (Scheme 6). The 3-cascade consists of vinylogous substitution, cyclization and 1,3-hydrogen shift. Again, the presumed elimination of water from the



Scheme 6. Quantitative solid-state 3-cascade of ninhydrin and methyl 3-aminocrotonate.

Table 1. Syntheses of **12** in mortar, ball-mill (bm), and solution.

12	Reaction conditions	Yield [%]	Yield in solution [%]	Ref.
a	mortar, 3 d at 80 °C	100	78	[8]
	bm, 1 h at 80 °C	100		
b	bm, 45 min, RT	100	91	[9]
c	mortar, 3 d	100	92	[10, 11]
	bm, 2 h, RT	100		
d	bm, 2 h, (water bath, 20 °C)	100	–	–
	mortar, 3 d, RT	100		
e	bm, 1 h, 60 °C	100	–	–

N/O-semiaminal **15** could not be obtained in a 4-cascade sequence in the solid state. Compound **15** had been synthesized in solution, but only in 82% yield.^[12] The structure of **15** is derived from the ¹H NMR data which exclude a symmetric diketo spiro[5,4]azaoctadien structure. DFT calculations at the B3LYP/6-31G* level give the imine tautomer (in brackets) 5.86 kcal mol^{−1} higher in energy than the enamine tautomer **15**.

AFM results: It appears interesting to study the influence of the molecular packing on the molecular movements in multistage cascade reactions in the solid state and to exclude (nano)liquid intermediate phases. Thus, six different crystal faces of **1** were studied with the AFM next to a reactant crystal of *o*-phenylenediamine (**7a**) on it. Ninhydrin (**1**) crystallizes in monoclinic prisms in the chiral space group *P*2₁.^[13] Hydrogen bonded double layers appear as principle motif. The O–H...O–H hydrogen bonds have O...O distance of 2.7981 Å, O–H...O=C of 2.805 Å.^[13] One of the carbonyl groups of **1** remains unbridged. There are no O–H hydrogen bonds between the double layers. The orientation of double layers determines the solid-state reactivity at the various faces. The molecules of **7a** migrate into the crystal of **1** as can be judged from a light yellow coloration. The (100)-face is not strongly present on the prismatic crystals of **1**, however, these cleave easily at that face and thus freshly cleaved (100)-surfaces were used in the measurements of Figure 1. A flat crystal of **7a** contacted well and was placed in [001]-direction from the AFM tip. The features of Figure 1 indicate only minor reactions on that face. The depth of the craters after 210 min does not exceed 20 nm and even the deepest crater after 380 min is only 65 nm deep. Evidently the reaction does not extend easily over the cleavage plane.

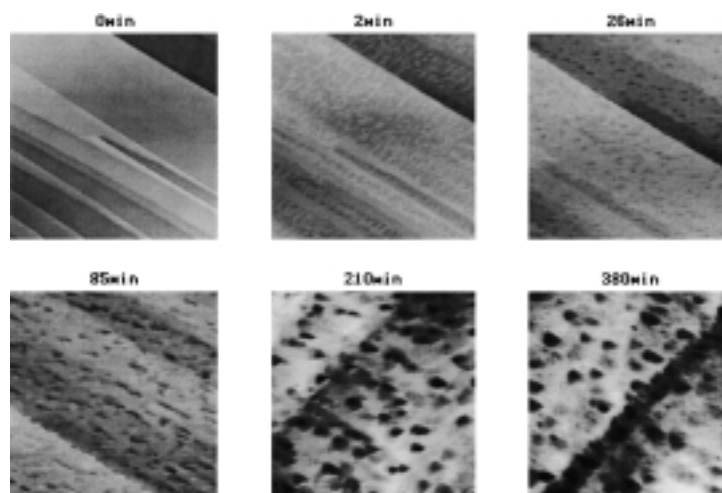


Figure 1. 9.5 μm AFM images of **1** on its (100)-cleavage plane at 0.1 mm distance from a crystal of **7a** on it after the times given, showing the formation of small craters that grow gradually. The z scale is 50 nm, the direction of preference runs along the [001]-direction (the scan direction was changed after 210 min).

The packing under the (100) double layers is shown in Figure 2. The molecules **7a** have to penetrate through the

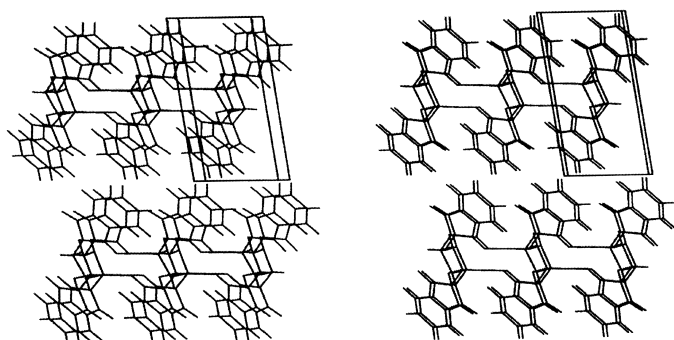


Figure 2. Stereoscopic view of the crystal packing of **1** on (010), but turned around y by 5° for a better view, showing the structure of the double layers (height ca. 11 nm) and the horizontal (100) cleavage plane; all hydrogen bonds are given.

double layers from the top, react and spread along the cleavage plane where the functional groups are shielded. It can thus be assumed that no rapid reaction occurs. The flat molecules **8a** appear to complex the water of the reaction while forming small craters around nucleation sites.

The behavior on the (10-1)-face of **1** that could be mounted after cutting the crystal across the major prism faces, is completely different. Figure 3 shows how the reaction with **7a** produces volcano type features all over the surface which grow together rapidly and assume heights of up to 1 μm in

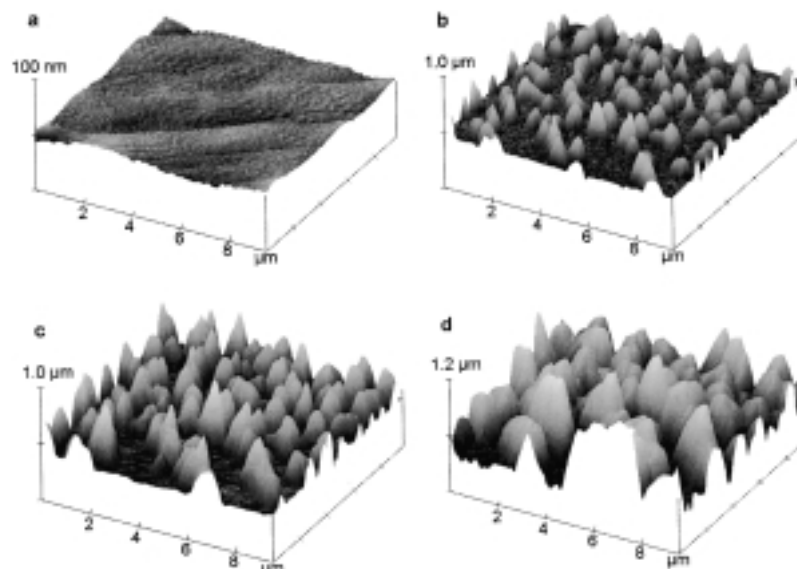


Figure 3. 9.5 μm AFM topographies on the (10-1)-face of **1** at 0.1 mm distance from a flat crystal of **7a**; a) fresh; b) after 2 min; c) after 15 min; d) after 60 min.

Figure 3 d. These densely packed hills grow slowly further to 1.35 μm after 3 h. Unlike the behavior in Figure 1 we have a strong transport of material above the (10-1)-surface. This behavior is derived from the crystal packing in Figure 4. The functional groups are available to **7a** for entering deeply into the crystal while reacting and spreading to the inclined cleavage planes from where apparently **8a** exits above the horizontal surface.

The major (1-10)- and (-1-10)-faces of **1** give the same type of features upon reaction with **7a**. Figure 5 shows the results on (1-10). Irrespective of the roughness in Figure 5 a, isolated island hills formed at the remarkably large distance of 0.5 mm by long-range molecular movements. These increased to edged mountains of considerable height without direction of preference (Figure 5 c, d) and grew to twice that height after 20 h.

The crystal packing in Figure 6 clearly indicates that the functional groups are available for reaction on the (1-10) surface. The product molecule **8a** can exit along the steep cleavage plane (100) and thus build the island mountains around nucleation sites while reacting molecules of **7a** enter the lattice. The molecular packing under the (-1-10) surface is the same as in Figure 6. It is thus not surprising that the same type of features ensue, as expected (this was shown at 0.3 mm distance). Furthermore, Figure 6 indicates that the packing under (-110) is different from the one on (1-10). It is the same as the packing under (110) and has the functional groups somewhat shielded by the skew benzo groups. Thus, at least a

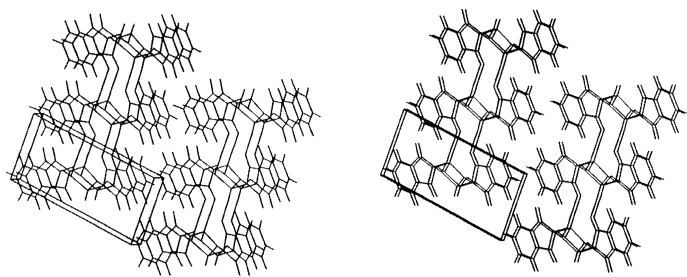


Figure 4. Stereoscopic view of the crystal packing of **1** with the (10-1)-face horizontal on top showing steep double layers; all hydrogen bonds are given.

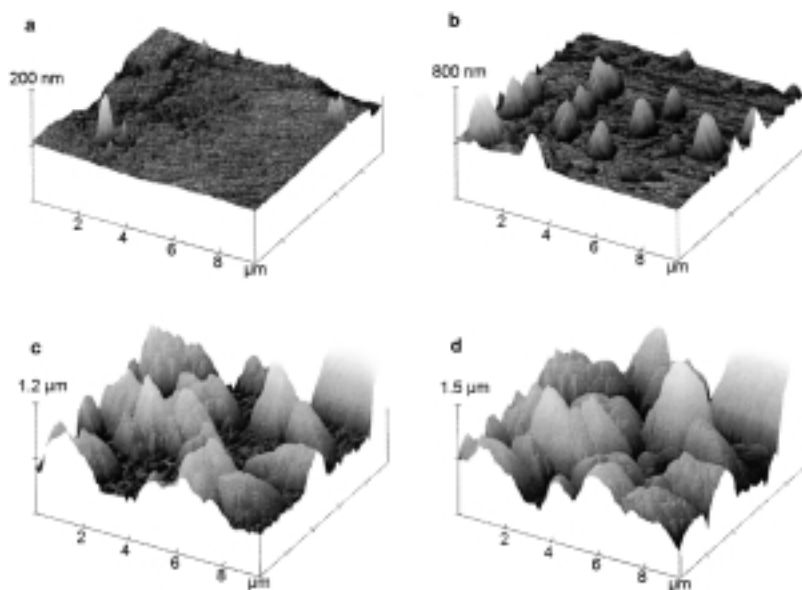


Figure 5. 9.5 μm AFM topographies on the (1-10)-face of **1** at 0.5 mm distance from a flat crystal of **7a**; a) fresh; b) after 15 min; c) after 2 h; d) after 4 h.

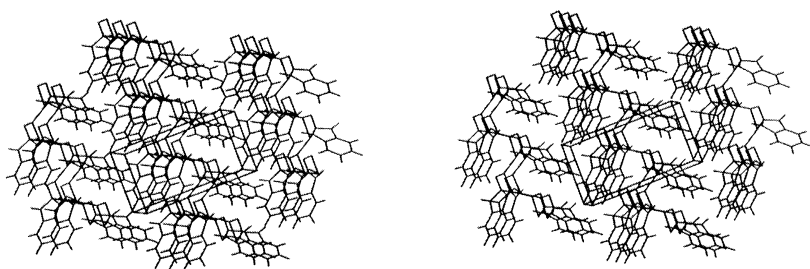


Figure 6. Stereoscopic packing diagram (crystal surfaces model) of **1** with (1-10) horizontal on top and (-110) horizontal at the bottom, showing the steep double layers. All hydrogen bonds are given.

different reactivity is expected and indeed, we assigned the more efficient feature formations to (1-10) and (-1-10) and the less efficient ones to the opposing (-110) and (110)-faces of the same crystal, respectively.

Figure 7 depicts the AFM results on the (-110) surface of **1**. The reaction of **7a** is indeed impeded, even though the initial natural surface is rather rough. Only few island features develop in the first 20 min (Figure 7b), but the reaction becomes fast at 90 min and similar features develop of comparable height than those in Figure 5, but their width remains smaller.

Again the behavior on (110) is closely comparable, due to the identical packing. After difficulties with its start, the rate approaches the one of the more favorable (-1-10)-face.

It appears, that the molecules **7a** have initially difficulties to enter the crystal on (-110) or (110) due to the impeding benzo groups except at very few nucleation centers. However, after considerable molecular movements the reaction gains in rate and the transport along the (100) cleavage plane is the same as on the opposite side of the crystal.

Discussion

Ninhydrin (**1**) is a rich source for waste-less quantitative solid-state cascades. Its melting point is quite high. Various reaction types were already shown with solution reactions which produce waste due to lower yield and workup requirements.

The unsurpassed performance of the presented solid-state cascades in stoichiometric runs is unusual and highly profitable in terms of sustainable synthesis with utmost efficiency in all respects. Their mechanistic basis was developed in numerous investigations of various types of solid state reactions using supermicroscopy (AFM and SNOM),^[1] and grazing incidence diffraction (GID),^[14] and correlations to crystal packings.^[1] Reaction cascades in the solid state are very complicated, however, they also profit from the general three-step solid state mechanism of 1) phase rebuilding, 2) phase transformation, and 3) crystal disintegration at any local sites and development. Unlike the gas/solid reactions step (2) does not occur suddenly in the solid/solid reactions

and it is hard to obtain the crystal disintegration with the studies at single crystals for technical reasons due to the very long distances. Nevertheless, the heights of the features at 0.5 mm distance show the high efficiency of the molecular migrations. Generally, step 3) and the generation of new contacts between the reacting crystals is attained by mechanical grinding, milling and other techniques.

The products of the condensation reactions of ninhydrin are preparatively useful building blocks which are now available without producing waste. The reactions are too slow to be completed in a mortar at moderate times, but proceed very

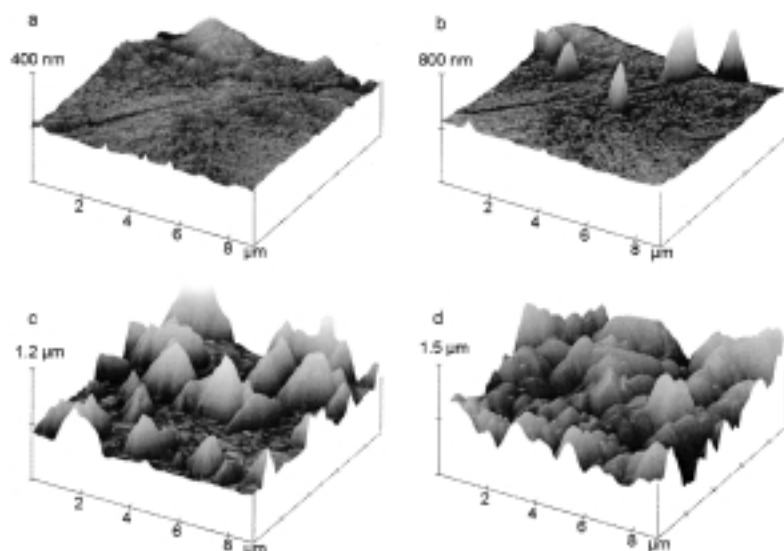


Figure 7. 9 μm AFM topographies on the (-110)-face of **1** at a 0.5 mm distance from a flat crystal of **7a** that was placed on it; a) fresh; b) after 20 min; c) after 2 h; d) after 4 h.

well in a ball-mill at milling times of less than one hour. We reported here on 12 quantitative and waste-free reaction cascades. Many more reaction cascades with ninhydrin **1** and diamines or diamides can be envisaged, as the crystal lattice of **1** appears very permissive to solid reaction partners.

Experimental Section

Melting points were determined with a Gallenkamp melting point apparatus and are uncorrected. Infrared (IR) spectra were recorded with a Perkin–Elmer 1720-X FT-IR spectrometer using potassium bromide pellets. All NMR spectra were taken at a Bruker WP 300 at 300 MHz (^1H) or 75 MHz (^{13}C). $\text{CDCl}_3/[\text{D}_6]\text{DMSO}$ mixtures contained up to 25% $[\text{D}_6]\text{DMSO}$. Mass spectra were obtained on a Finnigan MAT 212 System. DSC/TGA measurements were performed with a Perkin–Elmer DSC model 7 and TGA 7. The ball-mill was a Retsch MM 2000 swing mill with a 10 mL stainless steel double-walled beaker with fittings for circulating coolants. Two stainless steel balls with 12 mm diameter were used. Ball-milling was performed at 20–25 Hz frequency usually at room temperature (without circulating liquid the temperature did not rise above 30 °C). Water or methanol of the appropriate temperature was circulated for heating or cooling. Completeness of the solid-state reactions was checked by IR spectroscopy in KBr, product purity by m.p. and ^1H NMR spectroscopy. B3LYP (basis set 6-31G*) calculations with full geometry optimization were performed with the program TITAN, version 1.01 of Wavefunction, Inc., Irvine, USA. Single crystals of **1** were obtained by slow evaporation of solutions in water. The prisms selected had lengths of 3–4 mm and maximal widths of 2 mm. The AFM technique and the imaging have been described elsewhere.^[1]

Cleavage along the (100)-face of **1** is achieved by touching the (110)-face with a needle. Cutting across on the (110)-face required considerable pressure with a razor blade applied in the suitable direction. These cuts for (10-1)-faces were not always straight, but flat regions were chosen for the AFM measurements. Distances were judged by comparison with the crystal width that was measured with a slide gauge. Opposing (-1-10)/(110) and (1-10)/(-110)-faces were mounted from the same crystal species that was cut across with a razor blade so that the opposing surfaces could be mounted separately to the AFM. The faster reacting ones were assigned to (-1-10) and (1-10) for crystallographic reasons.

2-Hydroxy-2-(4,4-dimethyl-2,6-dioxocyclohexane-1-yl)-1H-indene-1,3(2H)-dione (3): Ninhydrin (**1**; 178 mg, 1.00 mmol) and dimedone (**2**; 140 mg, 1.00 mmol) were ball-milled for 1 h at room temperature. Pure **3** (300 mg,

100%) was obtained. M.p. 193–195 °C (decomp) (ref. [7]; 196–198 °C, decomp); ^1H NMR ($\text{CDCl}_3/[\text{D}_6]\text{DMSO}$): δ = 1.03 (s, 6H), 2.23 (s, 4H), 2.5–3.2 (brs, 2H), 7.60–7.80 (AA'BB', 2H), 7.80–8.00 (BB'AA', 2H).

1-Oxo-2-(1-pyrrolin-1-ylum)-1H-indene-3-olat (6): Ninhydrin (**1**; 356 mg, 2.00 mmol) and L-proline (**5**) (230 mg, 2.00 mmol) were ball-milled for 1 h. The teflon seal was tightened at 15 Nm to avoid dangerously high pressure. The water of the reaction was removed in a vacuum at 80 °C for 1 h to yield the title compound (421 mg, 99%). M.p. 239 °C (ref. [15]; 240 °C); IR (KBr): $\tilde{\nu}$ = 1663, 1625, 1577, 1408 cm^{-1} ; ^1H NMR ($\text{CDCl}_3/[\text{D}_6]\text{DMSO}$): δ = 2.20–2.34 (m, 2H), 3.00–3.12 (m, 2H), 4.83–4.95 (m, 2H), 7.46 (s, 4H), 9.24 (s, 1H); ^{13}C NMR ($\text{CDCl}_3/[\text{D}_6]\text{DMSO}$): δ = 17.61, 31.72, 57.31, 118.21 (2C), 130.19 (2C), 135.92, 150.82 (2C), 181.46 (2C), 213.78.

11H-Indeno[1,2-b]quinoxaline-11-one(8a): Ninhydrin (**1**) (356 mg, 2.00 mmol) and *o*-phenylenediamine (**7a**) (216 mg, 2.00 mmol) were ball-milled for 15 min at –5 °C. Compound **8a** (461 mg, 99%) was obtained after drying in a vacuum at 80 °C. M.p. 217–218 °C (ref. [6a]; 217–219 °C); IR (KBr): $\tilde{\nu}$ = 1732, 1605, 1571 cm^{-1} ; ^1H NMR (CDCl_3): δ = 7.56 (ψt , 1H), 7.77 (m, 3H), 7.90 (ψd , 1H), 8.09 (m, 2H), 8.20 (ψd , 1H); ^{13}C NMR ($\text{CDCl}_3/[\text{D}_6]\text{DMSO}$): δ = 122.2, 124.3, 129.3, 129.9, 131.1, 132.1, 132.2, 136.2, 136.5, 141.1, 142.2, 142.7, 148.9, 156.2, 189.5.

11H-6-Methylindeno[1,2-b]quinoxaline-11-one (8b): Ninhydrin (**1**; 178 mg, 1.00 mmol) and **7b** (122 mg, 1.00 mmol) were ball-milled for 1 h. After drying in a vacuum at 80 °C pure **8b** (264 mg, 100%) was obtained. M.p. 227 °C (ref. [6a]; 222–224 °C); IR (KBr): $\tilde{\nu}$ = 1726, 1568, 1193, 770 cm^{-1} ; ^1H NMR (CDCl_3): δ = 2.83 (s, 3H), 7.52–7.68 (m, 3H), 7.69–7.78 (ψt , 1H), 7.82–7.94 (ψd , 1H), 7.95–8.12 (ψt , 2H); ^{13}C NMR (CDCl_3): δ = 17.2, 122.3, 124.5, 129.4, 129.8, 132.1, 132.6, 136.5, 138.2 (2C), 141.8, 142.0, 142.7, 148.7, 155.4, 190.2.

11H-7,8-Dimethylindeno[1,2-b]quinoxaline-11-one (8c): Ninhydrin (**1**; 356 mg, 2.00 mmol) and **7c** (272 mg, 2.00 mmol) were ball-milled for 1 h. After drying in a vacuum at 80 °C pure **8c** (517 mg, 100%) was obtained. M.p. 248 °C; IR (KBr): $\tilde{\nu}$ = 1720, 1606, 1566 cm^{-1} ; ^1H NMR ($[\text{D}_6]\text{DMSO}$): δ = 2.49 (2s, 6H), 7.65 (ψt , 1H), 7.82 (m, 2H), 7.91 (s, 2H), 8.01 (ψd , 1H); ^{13}C NMR ($\text{CDCl}_3/[\text{D}_6]\text{DMSO}$): δ = 19.6, 19.9, 121.5, 123.7, 128.4, 129.9, 131.5, 135.7, 136.0, 140.2, 140.7, 141.0, 141.2, 142.9, 147.6, 155.4, 189.5; HR-MS (CI, isobutane): calcd for $\text{C}_{17}\text{H}_{12}\text{N}_2\text{O}+\text{H}$: 261.1040; found: 261.1041.

10a-Hydroxyindeno[2,1-b]benz[1,4]thiazin-11(10aH)-one (10): Ninhydrin (**1**; 356 mg, 2.00 mmol) and *o*-aminothiophenol hydrochloride (**9**) (323 mg, 2.00 mmol) were ball-milled for 1 h. The solid product was washed with saturated NaHCO_3 solution and dried to obtain pure **10** (529 mg, 99%). M.p. 227 °C (ref. [7]; 228 °C); IR (KBr): $\tilde{\nu}$ = 1733, 1639, 1594 cm^{-1} ; ^1H NMR ($\text{CDCl}_3/[\text{D}_6]\text{DMSO}$): δ = 7.24 (ψt , 1H), 7.33 (ψt , 1H), 7.46 (ψd , 1H), 7.58 (s, OH), 7.65 (ψd , 1H), 7.79 (ψt , 1H), 7.93 (m, 2H), 8.20 (ψd , 2H); ^{13}C NMR ($\text{CDCl}_3/[\text{D}_6]\text{DMSO}$): δ = 119.5, 122.2, 122.9, 125.2 (2C), 126.3, 127.5, 131.9, 133.6, 135.6, 140.8 (2C), 141.6, 154.0, 193.6.

3a,8a-Dihydroxy-1,3,3a,8a-tetrahydroindeno[1,2-d]imidazole-2,8-dione (12a): Ninhydrin (**1**; 534 mg, 3.00 mmol) and urea (**11a**) (180 mg, 3.00 mmol) were ball-milled at 80 °C for 1 h. After drying at 140 °C for 5 min in a vacuum pure **12a** (696 mg, 100%) was obtained. M.p. 218 °C (decomp) (ref. [8]; 218–220 °C); IR (KBr): $\tilde{\nu}$ = 3347, 1728, 1692, 1604, 1413, 1116 cm^{-1} ; ^1H NMR ($[\text{D}_6]\text{DMSO}$): δ = 6.39 (s, 1H), 6.50 (s, 1H), 7.57 (ψt , 1H), 7.78 (ψt , 2H), 7.85 (s, 2H), 8.00 (s, 1H); ^{13}C NMR ($[\text{D}_6]\text{DMSO}$): δ = 86.6 (2C), 123.4, 125.1, 130.0, 132.1, 136.6, 152.0, 156.7, 197.9.

3a,8a-Dihydroxy-2-thioxo-2,3,3a,8a-tetrahydro-1H-indeno[1,2-d]imidazole-8-one (12b): Ninhydrin (**1**; 178 mg, 1.00 mmol) and thiourea (**11b**) (76 mg, 1.00 mmol) were ball-milled for 45 min. Pure **12b** (236 mg, 100%) was obtained. M.p. 220 °C (decomp) (ref. [9]; 240–242 °C); IR (KBr): $\tilde{\nu}$ = 3310, 1728, 1510, 1107, 615 cm^{-1} ; ^1H NMR ($\text{CDCl}_3/[\text{D}_6]\text{DMSO}$): δ = 6.40 (brs, 1H), 6.60 (brs, 1H), 7.50–7.60 (ψt , 1H), 7.70–7.95 (m, 3H), 9.13 (brs,

1H), 9.62 (brs, 1H); ¹³C NMR (CDCl₃/[D₆]DMSO): δ = 88.6, 89.5, 122.7, 124.2, 129.1, 131.8, 135.4, 149.5, 177.7, 194.8.

3a,8a-Dihydroxy-1,3-dimethyl-1,3,3a,8a-tetrahydroindeno[1,2-d]imidazole-2,8-dione (12c): Ninhydrin (**1**; 178 mg, 1.00 mmol) and *N,N'*-dimethylurea (**11c**) (88 mg, 1.00 mmol) were ball-milled for 2 h. Pure **12c** (248 mg, 100%) was obtained. M.p. 248 °C (ref. [11]: 247–251 °C); IR (KBr): $\tilde{\nu}$ = 3308, 3153, 1732, 1686, 1604, 1490, 1418, 1400 cm⁻¹; ¹H NMR (CDCl₃/[D₆]DMSO): δ = 2.82 (s, 3H), 2.88 (s, 3H), 6.00–6.30 (brs, 1H), 6.35–6.60 (brs, 1H), 7.40–7.55 (m, 1H), 7.65–7.78 (m, 3H); ¹³C NMR (CDCl₃/[D₆]DMSO): δ = 23.5, 23.8, 85.7, 86.7, 123.2, 123.7, 129.1, 131.8, 135.1, 148.0, 154.2, 194.6.

3a,8a-Dihydroxy-1,3-dimethyl-2-thioxo-2,3,3a,8a-tetrahydro-1H-indeno[1,2-d]imidazole-8-one (12d): Ninhydrin (**1**; 178 mg, 1.00 mmol) and *N,N'*-dimethylthiourea (**11d**) (104 mg, 1.00 mmol) were ball-milled at 20 °C for 2 h. Pure **12d** (264 mg, 100%) was obtained. M.p. 219 °C (decomp); IR (KBr): $\tilde{\nu}$ = 3327, 3215, 1700, 1600, 1467, 1381, 1303, 1224 cm⁻¹; ¹H NMR (CDCl₃/[D₆]DMSO): δ = 3.25 (s, 3H), 3.32 (s, 3H), 6.40–6.70 (brs, 1H), 6.70–6.90 (brs, 1H), 7.50–7.62 (m, 1H), 7.72–7.88 (m, 3H); ¹³C NMR (CDCl₃/[D₆]DMSO): δ = 28.0, 28.4, 88.5, 90.1, 123.8, 124.1, 129.8, 132.4, 135.8, 147.5, 177.9, 193.6; HR-MS (CI, isobutane): calcd for C₁₂H₁₂N₂O₃S+H: 265.0674; found: 265.0681.

3a,8a-Dihydroxy-1,3-diphenyl-2-thioxo-2,3,3a,8a-tetrahydro-1H-indeno[1,2-d]imidazole-8-one (12e): Ninhydrin (**1**; 178 mg, 1.00 mmol) and *N,N'*-diphenylthiourea (**11e**) (228 mg, 1.00 mmol) were ball-milled at 60 °C for 1 h. Pure **12e** (388 mg, 100%) was obtained. M.p. 212 °C (decomp); ¹H NMR (CDCl₃/[D₆]DMSO): δ = 6.85–6.95 (m, 1H), 7.10–7.20 (brs, 1H), 7.30–7.53 (m, 11H), 7.55–7.65 (m, 2H), 7.80–7.90 (m, 1H); ¹³C NMR (CDCl₃/[D₆]DMSO): δ = 90.4, 92.0, 123.6, 125.0, 127.6, 127.7, 127.9, 130.1, 132.4, 135.4, 135.8, 136.0, 147.6, 179.8, 193.4; HR-MS (EI): calcd for C₂₂H₁₆N₂O₃S: 388.0882; found: 388.0885.

3a,8a-Dihydroxy-2-methyl-8-oxo-3,3a,8,8a-tetrahydro-3-aza-cyclopent[a]indene-1-carboxylic methyl ester (15): Ninhydrin (**1**; 356 mg, 2.00 mmol) and methyl 3-aminocrotonate (**14**) (230 mg, 2.00 mmol) were ball-milled for 1 h. The solid was dried in a vacuum at 80 °C to yield **15** (545 mg, 99%). M.p. 201 °C (ref. [12]: 201–202 °C); IR (KBr): $\tilde{\nu}$ = 3518, 3437, 3313, 1706, 1644 cm⁻¹; ¹H NMR (CDCl₃/[D₆]DMSO): δ = 2.05 (s, 3H), 3.50 (s, 3H), 5.38 (s, OH), 6.35 (s, OH), 7.48–7.60 (ψt, 1H), 7.65 (ψd, 2H), 7.78 (ψd, 1H), 8.80 (s, 1H); ¹³C NMR (CDCl₃/[D₆]DMSO): δ = 14.4, 49.5, 85.2, 91.5, 94.7, 122.5, 124.7, 129.8, 134.2, 134.7, 149.7, 160.0, 165.5, 198.9.

Acknowledgement

This work was supported by the Deutsche Forschungsgemeinschaft and the Fonds der Chemischen Industrie. We thank Dr. W. Saak for the Miller indices of ninhydrin and Mrs. Ludmila Hermann for her skillful help in the experimental work.

- [1] G. Kaupp, in *Comprehensive Supramolecular Chemistry*, Vol. 8 (Ed.: J. E. D. Davies), Elsevier, Oxford, **1996**, pp. 381–423.
- [2] N. P. Peet, E. W. Huber, J. C. Huffman, *J. Heterocycl. Chem.* **1995**, 32, 33.
- [3] F. Campagna, A. Carotti, G. Casini, M. Ferappi, *Gazz. Chim. Ital.* **1983**, 113, 507.
- [4] A. W. Johnson, D. J. McCaldin, *J. Chem. Soc.* **1958**, 817.
- [5] M. F. Aly, H. Ardill, R. Grigg, S. Leong-Ling, S. Rajviroongit, S. Surendrakumar, *Tetrahedron Lett.* **1987**, 28, 6077.
- [6] a) L. W. Deady, J. Desneves, A. C. Ross, *Tetrahedron* **1993**, 49, 9823; b) S. Ruhemann, *J. Chem. Soc.* **1910**, 97, 1438.
- [7] A. Schöenberg, E. Singer, G.-A. Hoyer, D. Rosenberg, *Chem. Ber.* **1977**, 110, 3954.
- [8] R. Caputo, C. Ferreri, G. Palumbo, V. Adovasio, M. Nardelli, *Gazz. Chim. Ital.* **1987**, 117, 731.
- [9] N. Chatterjee, R. A. Stephani, C. H. Strom, *J. Pharm. Sci.* **1980**, 69, 1431.
- [10] R. Shapiro, N. Chatterjee, *J. Org. Chem.* **1970**, 35, 447.
- [11] P. A. Crooks, T. Deeks, *Chem. Ind.* **1975**, 793.
- [12] N. Chatterjee, R. Shapiro, S.-G. Quo, R. A. Stephani, *Tetrahedron Lett.* **1975**, 30, 2535.
- [13] R. C. Medrud, *Acta Crystallogr. Sect. B* **1969**, 25, 213.
- [14] A. Herrmann, G. Kaupp, T. Geue, U. Pietsch, *Mol. Cryst. Liq. Cryst.* **1997**, 293, 261.
- [15] A. Schwarz, G. Uray, H. Junek, *Liebigs Ann. Chem.* **1980**, 1919.

Received: July 16, 2001 [F3417]